GFZ
Helmholtz-Zentrum
POTSDAM

Originally published as:

Yu, X., Yuan, Z., Huang, S., Yao, F., Wang, D., Funsten, H. O., Wygant, J. R. (2018): Excitation of O+ Band EMIC Waves Through H+ Ring Velocity Distributions: Van Allen Probe Observations. - *Geophysical Research Letters*, *45*, 3, pp. 1271—1276.

DOI: http://doi.org/10.1002/2018GL077109

AGU PUBLICATIONS

Geophysical Research Letters

RESEARCH LETTER
10.1002/2018GL077109

Key Points:
- In situ observations were used to investigate the excitation of O^+ band EMIC waves
- Combination of observations and theory analysis demonstrates that RC protons with ring velocity distributions can drive O^+ band EMIC waves
- This paper demonstrates those previous theoretical predictions of excitation for O^+ band EMIC waves

Supporting Information:
- Supporting Information S1

Correspondence to:
Z. Yuan,
y_zgang@vip.163.com

Citation:
Yu, X., Yuan, Z., Huang, S., Yao, F., Wang, D., Funsten, H. O., & Wygant, J. R. (2018). Excitation of O^+ band EMIC waves through H^+ ring velocity distributions: Van Allen Probe observations. *Geophysical Research Letters, 45*, 1271–1276. https://doi.org/10.1002/2018GL077109

Received 10 JAN 2018
Accepted 28 JAN 2018
Accepted article online 2 FEB 2018
Published online 15 FEB 2018

©2018. American Geophysical Union. All Rights Reserved.

Excitation of O^+ Band EMIC Waves Through H^+ Ring Velocity Distributions: Van Allen Probe Observations

Xiongdong Yu[1], Zhigang Yuan[1], Shiyong Huang[1], Fei Yao[1], Dedong Wang[2], Herbert O. Funsten[3], and John R. Wygant[4]

[1]School of Electronic Information, Wuhan University, Wuhan, China, [2]GFZ German Research Center for Geosciences, Potsdam, Germany, [3]Los Alamos National Laboratory, Los Alamos, NM, USA, [4]School of Physics and Astronomy, University of Minnesota, Minneapolis, MN, USA

Abstract A typical case of electromagnetic ion cyclotron (EMIC) emissions with both He^+ band and O^+ band waves was observed by Van Allen Probe A on 14 July 2014. These emissions occurred in the morning sector on the equator inside the plasmasphere, in which region O^+ band EMIC waves prefer to appear. Through property analysis of these emissions, it is found that the He^+ band EMIC waves are linearly polarized and propagating quasi-parallelly along the background magnetic field, while the O^+ band ones are of linear and left-hand polarization and propagating obliquely with respect to the background magnetic field. Using the in situ observations of plasma environment and particle data, excitation of these O^+ band EMIC waves has been investigated with the linear growth theory. The calculated linear growth rate shows that these O^+ band EMIC waves can be locally excited by ring current protons with ring velocity distributions. The comparison of the observed wave spectral intensity and the calculated growth rate suggests that the density of H^+ rings providing the free energy for the instability has decreased after the wave grows. Therefore, this paper provides a direct observational evidence to the excitation mechanism of O^+ band EMIC waves: ring current protons with ring distributions provide the free energy supporting the instability in the presence of rich O^+ in the plasmasphere.

Plain Language Summary Electromagnetic ion cyclotron (EMIC) waves can play an important role in the dynamics of the magnetosphere. Excitation of EMIC waves is usually considered through temperature-anisotropy of ring current hydrogen ions. Considering that EMIC waves in O+ band have different properties in comparison with those in H+ and He+ bands, theoretical prediction has been proposed that O+ band EMIC waves might be excited by protons with ring velocity distributions, which is different to the excitations of H+ or He+ band EMIC waves through temperature-anisotropy of ring current protons. However, direct observational evidence supporting this theoretical result has not been provided yet. In this letter, we report a typical case of excitation of O+ band EMIC waves. Combining of observations and theory analysis, we demonstrate that ring current protons with ring velocity distributions can drive O+ band EMIC waves, which is in accordance with previous theoretical predictions.

1. Introduction

Electromagnetic ion cyclotron (EMIC) waves are usually observed in the terrestrial magnetosphere. These waves are often with predominately left-hand polarization and small wave normal angles in their source regions (Allen et al., 2015; Anderson et al., 1992; Liu et al., 2012; Loto'aniu et al., 2005; Min et al., 2012). After propagating away from their source regions, these waves would have large wave normal angles and linear polarization, because of the refraction of the background magnetic field (Chen et al., 2014). Due to the presence of heavier ions (He^+ and O^+) than H^+ in the cold background plasma, EMIC waves are often observed in three distinct bands: H^+ band, He^+ band, and O^+ band. Generally, H^+ band EMIC waves have angular frequencies (ω) between the angular gyrofrequencies of H^+ and He^+ ($\Omega_{He+} < \omega < \Omega_{H+}$), He^+ band EMIC waves have angular frequencies between the angular gyrofrequencies of He^+ and O^+ ($\Omega_{O+} < \omega < \Omega_{He+}$), while O^+ band EMIC waves have angular frequencies below the angular gyrofrequencies of O^+ ($\omega < \Omega_{O+}$), where Ω_{H+}, Ω_{He+}, and Ω_{O+} are angular gyrofrequencies of H^+, He^+, and O^+, respectively.

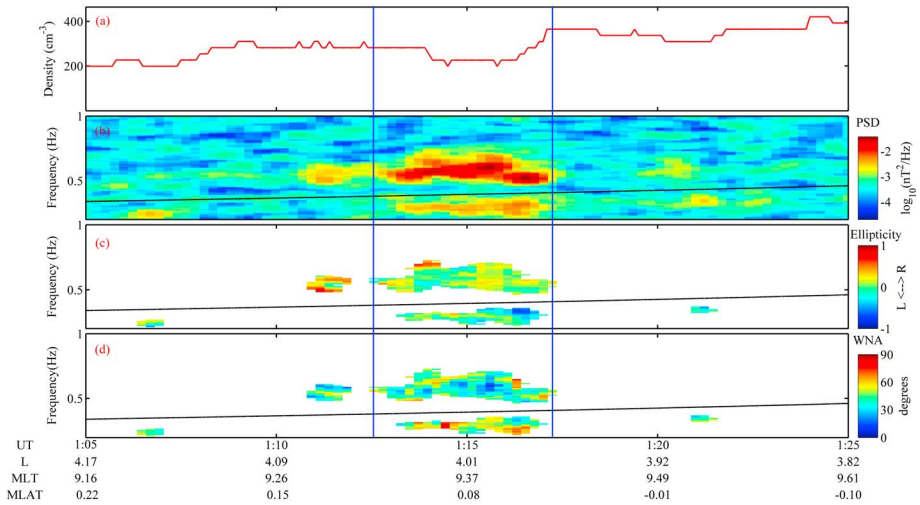

Figure 1. An overview of the electromagnetic ion cyclotron wave event observed by Van Allen Probe A during 01:05:00–01:25:00 UT on 14 July 2014. (a) Electron density profile. (b) Wave power spectrum density (PSD). (c) Ellipticity. (d) Wave normal angles. The black curves in panels (c) and (d) denote the local gyrofrequencies of O^+ (f_{O+}). The two vertical blue lines denote the interval of interest, where electromagnetic ion cyclotron waves in He^+ and O^+ bands are observed.

It has been demonstrated that EMIC waves can play an important role in the dynamic evolution of the magnetospheric processes, such as energizing cold electrons and ions (Yuan et al., 2014, 2016; Zhang et al., 2010), leading to precipitation of ring current ions (Yuan et al., 2010, 2012), making rapid loss of radiation belt electrons through pitch angle scattering (Usanova et al., 2014; Yuan et al., 2013), etc. Therefore, uncovering the excitation mechanism of EMIC waves is of significance for understanding magnetospheric dynamics.

EMIC waves in H^+ and He^+ bands are thought to be excited by ring current ions with temperature-anisotropy velocity distributions (e.g., Cornwall, 1965; Kennel & Petschek, 1966; Kozyra et al., 1984; Lee et al., 2017; Xue et al., 1993; Yuan et al., 2016), which has been verified by satellite observations (e.g., Min et al., 2015). Considering that EMIC waves in O^+ band have different properties in comparison with those in H^+ and He^+ bands, that is, O^+ band EMIC waves often have large wave normal angles and left-hand or/and linear polarization (Saikin et al., 2015; Yu et al., 2015), Yu et al. (2016) have used linear growth theory to predict that O^+ band EMIC waves might be excited by protons with ring velocity distributions ($\partial f_\perp/\partial v_\perp > 0$, where $f_\perp = f(v_\perp, v_{//} = 0)$ is the perpendicular velocity distribution). However, direct observational evidence supporting this theoretical result has not been provided yet.

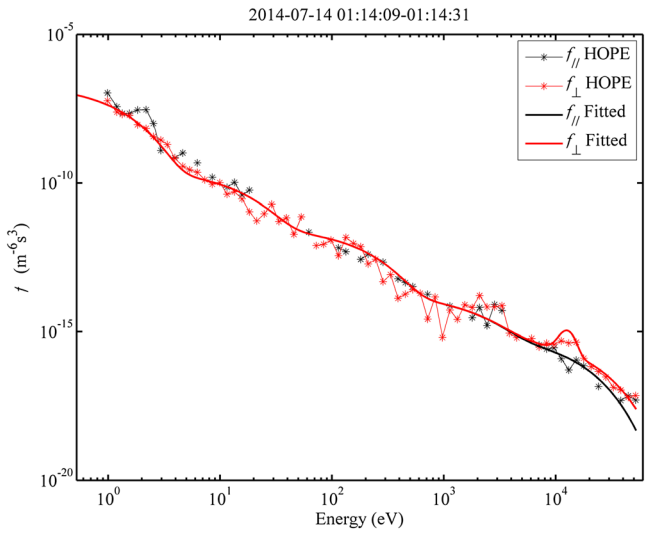

Figure 2. The observed and fitted H^+ phase space distributions. The black and red curves with asterisk markers denote the observed parallel ($f_{//}$) and perpendicular ($f_\perp$) components, respectively, while the bold black and red curves denote the fitted $f_{//}$ and $f_\perp$, respectively.

In this paper, we report a typical case of EMIC emissions with both He^+ band and O^+ band waves observed by Van Allen Probe A on 14 July 2014. Next, using the in situ observation of plasma environment and particle data, we have calculated the linear growth rate of O^+ band EMIC waves and found that these observed O^+ band EMIC waves can be locally excited by ring current protons with ring velocity distributions. Finally, the evolution of the density of the H^+ ring with wave growth is discussed.

2. Observations

The upper hybrid resonant frequencies, identified from the wave spectrum provided by the Electric and Magnetic Field Instrument Suite and Integrated Science (Kletzing et al., 2013), are utilized to infer the plasma density (n_e) (Kurth et al., 2015). We also extract the perturbed magnetic field (ΔB_x, ΔB_y, and ΔB_z) from the 64 sample/s magnetic field vector data

Table 1
Proton Components Used to Model the Proton Phase Space Distributions

Components	n (cm^{-3})	$T_{//}$ (eV)	$T_{\perp}$ (eV)	E_r (eV)[a]
1	98.821	0.6	0.6	0
2	0.100	8	8	0
3	0.050	100	100	0
4	0.010	1,100	1,100	0
5	0.010	31.15×10^3	120	12.54×10^3
6	0.009	7.0×10^3	10.0×10^3	0

[a] $E_r = \frac{1}{2} m_h V_r^2$ is the energy parameter relative to the ring speed V_r (Yu et al., 2016).

attained from Electric and Magnetic Field Instrument Suite and Integrated Science and transform these perturbed magnetic field into a field-aligned coordinate system to get the parallel component ($\Delta B_{//}$) and the other two perpendicular perturbed components ($\Delta B_{\perp 1}$ and $\Delta B_{\perp 2}$) (Yu et al., 2017; Yuan et al., 2016). Then one of the perpendicular components ($\Delta B_{\perp 1}$) is used to acquire the wave power spectrum density (PSD) by the Fast Fourier transformation, and the ellipticity (ε) and wave normal angles (θ) are obtained through the singular value decomposition analysis of $\Delta B_{//}$, $\Delta B_{\perp 1}$, and $\Delta B_{\perp 2}$ (Santolík et al., 2003). Moreover, the differential fluxes of H^+ attained from the Helium, Oxygen, Proton, and Electron (HOPE) mass spectrometer (Funsten et al., 2013) are exploited to obtain the H^+ phase space distributions (f), from which proton ring velocity distributions are identified.

Figure 1 shows an overview of the EMIC wave event observed by Van Allen Probe A during 01:05:00–01:25:00 UT on 14 July 2014. The plasma density (n_e), wave PSD, ellipticity (ε), and wave normal angles (θ) are displayed in Figures 1a–1d, respectively. The black curves in Figures 1c and 1d denote the local gyrofrequencies of O^+ (f_{O+}). In the interval of interest, denoted by the two vertical blue lines, EMIC waves are observed in the morning sector (MLT ≈ 9.37 hr) on the equator (MLAT ~ 0°) inside the plasmasphere ($L \approx 4$, $n_e \approx 200$ cm^{-3}), in which region O^+ band EMIC waves prefer to appear (Yu et al., 2015, 2016). These observed EMIC waves have two-band structures, with one band above f_{O+} and the other below f_{O+}. The emissions with frequencies above f_{O+} have linear but slightly right-hand polarization (ε ~ 0) and small wave normal angles ($\theta \leq 40°$) so that they are identified as He^+ band EMIC waves, while those emissions with frequencies below f_{O+}, linear to left-hand polarization ($\varepsilon < \sim 0$), and large normal angles ($\theta \geq 50°$) are O^+ band EMIC waves. The excitation of the He^+ band EMIC waves is discussed in the supporting information, and we will focus only on the O^+ band EMIC waves with large normal angles hereinafter.

In order to investigate the excitation of O^+ band EMIC waves, we have checked the observed H^+ phase space distributions. The parallel ($f_{//}$) and perpendicular ($f_{\perp}$) components of the observed H^+ phase space distributions during 01:14:09–01:14:31 UT are displayed as black and red curves with asterisk markers in Figure 2, respectively. Both two components are shown as a function of energy. As shown in Figure 2, the observed H^+ is mainly isotropic in the energy range below 10 keV, while an H^+ ring (a positive gradient on $f_{\perp}$) is observed at energies about 12 keV. The H^+ ring is also called as H^+ with a ring velocity distribution. It is worth noting that the H^+ ring at energies about 12 keV occurred during the whole time interval, where O^+ band EMIC waves are observed, rather than the only time stamp shown here. A best-Gaussian-ring-distribution fitting is performed to estimate this H^+ ring (Yuan et al., 2017), while the rest is fitted with Maxwellian distributions. As a result, the fitted parameters are exhibited in Table 1, and the fitted parallel and perpendicular phase space distributions are denoted by the bold black and red curves in Figure 2, respectively. Note that there is also a minor bump at energies between 1 and 3 keV, but we have modeled it as a Maxwellian distribution. This is because that even if it is modeled as an H^+ ring, it make slight difference to our results due to a small ring speed (Yu et al., 2016). Moreover, we have assumed that besides the multicomponet H^+, the background plasma consists of cold electron, He^+, and O^+, whose temperatures are 2, 0.6, and 1 eV, respectively (Olsen et al., 1987; Yu et al., 2016). The HOPE measurement covers the dominant ion species (H^+, He^+, and O^+), and electrons with energies from ~1 to 50 keV relative to the spacecraft potential (Funsten et al., 2013). In fact, due to the spacecraft potential of ~1.2 eV observed by the Electric Field and Waves instruments (Wygant et al., 2013) during the interval of O^+ band EMIC waves, the HOPE cannot detect many of the cold ions <2 eV (Yuan

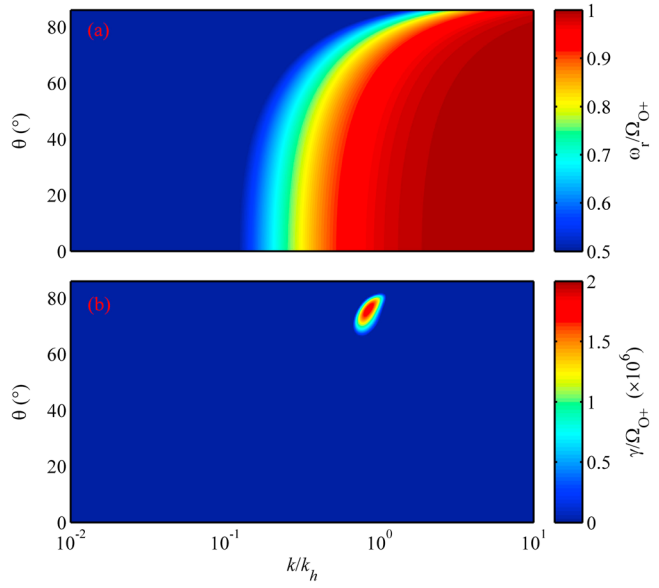

Figure 3. The solved wave frequency and linear growth rate normalized to Ω_{O+}, that is, ω_r/Ω_{O+} and γ/Ω_{O+}, as a function of wave normal angles (θ) and normalized wave numbers (k/k_h).

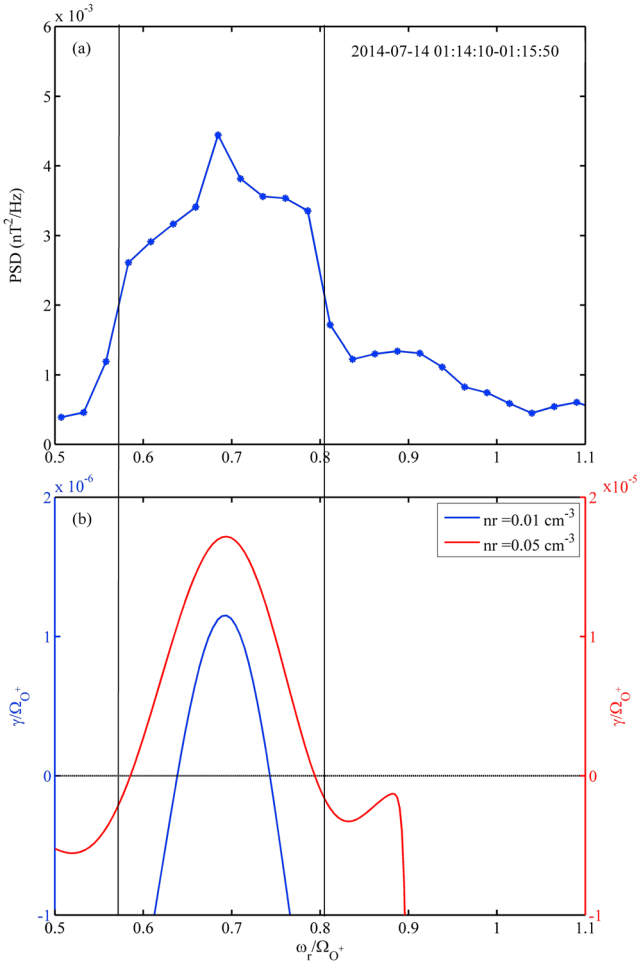

Figure 4. Comparison of the observed wave power spectrum density (PSD) and the calculated linear growth rate as a function of the normalized frequency. (a) The observed wave PSD. (b) The linear growth rate for n_r = 0.01 cm^{-3} (blue) and 0.05 cm^{-3} (red), where n_r is the density of the H^+ rings.

et al., 2016). Since these waves are observed during the last recovery phase of a magnetic storm (not shown) during which background plasma with rich O^+ prefers to occur (e.g., H^+ : He^+ : O^+ = 45% : 10% : 45% in Nosé et al., 2011), and Yu et al. (2016) have predicted that O^+ band EMIC waves prefer to occur in a rich-O^+ background plasma, the ion compositions of H^+, He^+, and O^+ in the background plasma are set to be 45%, 10%, and 45%, respectively. Note that the observed magnetic field is 445 nT, and the plasma density is 220 cm^{-3}. Linear growth theory will be utilized to verify the wave instabilities, and the results are shown in the discussion section.

3. Discussions

With the plasma parameters above, the linear growth rate (γ) of O^+ band EMIC waves with different wave normal angles (θ) can be calculated through the equations proposed in Yu et al. (2016). The real frequency (ω_r) is solved from the cold plasma dispersion relation $D^{(0)}(\omega_r,k) = 0$ in Kennel (1966). The solved ω_r and γ normalized to Ω_{O+}, that is, ω_r/Ω_{O+} and γ/Ω_{O+}, are shown as a function of wave normal angles (θ) and normalized wave numbers (k/k_h) in Figures 3a and 3b, respectively. Here $k_h = \sqrt{e^2 n_e/(\varepsilon_0 m_h)}/c$ is the inverse of the H^+ inertial length, where m_h is the proton mass, ε_0 is the vacuum dielectric constant, and c is the speed of light. The theoretical ellipticity of O^+ band EMIC waves is slightly less than zero (not shown), which is consistent with the observations (cf. Figure 1d). As clearly shown in Figure 3b, positive growth rate ($\gamma > 0$) occurs only for large wave normal angles ($65° < \theta < 80°$), which indicates that only the instability with large θ can grow up. It is different with the instability driven by hot H^+ with temperature-anisotropy bi-Mawellian distributions. The latter would have positive growth rate for small normal angles (see Figure 1c in Yu et al. (2016)), and usually thought to be the candidate generation mechanism of H^+ and He^+ band EMIC waves. However, O^+ band EMIC waves are observed to have large wave normal angles (see Figure 1). The calculated growth rate shown in Figure 3 indicates that the observed O^+ band EMIC waves might be excited by ring current H^+ with ring velocity distributions.

To compare satellite observations and the theoretical calculation in details, the wave PSD observed during 01:14:10–01:14:50 UT and the normalized growth rate (γ/Ω_{O+}) at θ = 80° are illustrated as blue curves in Figures 4a and 4b, respectively. In both panels, the abscissa is the normalized angular frequency (ω/Ω_{O+}). Note that the comparison presented here is only to show the possibility that the observed waves can be excited by the instability with positive growth rates in specified wave modes and frequency band. The study of the saturated wave amplitudes would involve more than linear growth theory presented here. As shown in Figure 4b, the growth rate peaks at a normalized frequency about 0.7, which is consistent with the observed wave PSD. On the other hand, the unstable frequency interval ($0.64 < \omega/\Omega_{O+} < 0.74$), indicated by positive growth rate, is somewhat narrower than the frequency width of the observed O^+ band EMIC waves (denoted by the two black vertical lines). This difference needs some further explanation, and we try to interpret it as a result of the evolution of the H^+ ring during the wave growth as follows.

In fact, one assumption has been made for linear growth theory that the zero-order particle distribution is affected slightly as the instability grows up. However, since the H^+ ring provides the free energy supporting the wave growth, when waves have attained certain energy so as to be available for satellite observations, the distribution of H^+ ring might have developed, which has been demonstrated in Min and Liu (2016). Therefore, we assume the initial density of the H^+ ring n_r to be 0.05 cm^{-3} (a larger value, e.g., n_r = 0.1 cm^{-3}, would get essentially same results), which would decrease to the observed density (0.01 cm^{-3}) after waves grow, and

check the corresponding growth rate. The result is displayed as the red curve in Figure 4b. Obviously, the calculated growth rate for n_r = 0.05 cm^{-3} is substantially consistent with the observed PSD of O^+ band EMIC waves, in both the peak and frequency width. It is suggested that the density of the H^+ ring might have decreased as wave grows up.

4. Conclusions

In this paper, a typical case of EMIC emissions with both He^+ band and O^+ band waves observed by Van Allen Probe A on 14 July 2014 is reported. The observed He^+ band EMIC waves have linear polarization and propagate quasi-parallelly along the background magnetic field, while the O^+ band ones are of linear and left-hand polarization and propagating obliquely. Using the linear growth theory as well as the in situ plasma environment and particle data, we have demonstrated that these observed O^+ band EMIC waves can be excited locally by ring current H^+ with ring velocity distributions, which is in accordance with previous theoretical predictions (Yu et al., 2016). Therefore, this paper provides a direct observational evidence of the excitation of O^+ band EMIC waves. On the other hand, the observed wave spectral intensity has been compared with the calculated growth rate, and the result suggests that as the H^+ ring provides the free energy supporting the instability, the density of the H^+ ring has decreased after the wave grows. This evolution of the H^+ ring would be studied in more details in the future via computer particle simulations.

Acknowledgments
The Van Allen Probes data are available at the Web http://www.rbsp-ect.lanl.gov/data_pub/, http://www.space.umn.edu/rbspefw-data/ and http://emfisis.physics.uiowa.edu/data/index. This work is supported by the National Natural Science Foundation of China (41374168, 41521063, and 41174140) and Program for New Century Excellent Talents in University (NCET-13-0446). Both the data and input files necessary to reproduce the experiments are available from the authors upon request (y_zgang@vip.163.com).

References

Allen, R. C., Zhang, J.-C., Kistler, L. M., Spence, H. E., Lin, R.-L., Klecker, B., et al. (2015). A statistical study of EMIC waves observed by Cluster: 1. Wave properties. *Journal of Geophysical Research: Space Physics*, *120*, 5574–5592. https://doi.org/10.1002/2015JA021333

Anderson, B. J., Erlandson, R. E., & Zanetti, L. J. (1992). A statistical study of Pc1–2 magnetic pulsations in the equatorial magnetosphere: 2. Wave properties. *Journal of Geophysical Research*, *97*(A3), 3089–3101. https://doi.org/10.1029/91JA02697

Chen, L., Jordanova, V. K., Spasojevic, M., Thorne, R. M., & Horne, R. B. (2014). Electromagnetic ion cyclotron wave modeling during the Geospace Environment Modeling challenge event. *Journal of Geophysical Research: Space Physics*, *119*, 2963–2977. https://doi.org/10.1029/2013JA019595

Cornwall, J. M. (1965). Cyclotron instabilities and electromagnetic emissions in the ultra low frequency and very low frequency ranges. *Journal of Geophysical Research*, *70*(1), 61–69. https://doi.org/10.1029/JZ070i001p00061

Funsten, H. O., Skoug, R. M., Guthrie, A. A., MacDonald, E. A., Baldonado, J. R., Harper, R. W., et al. (2013). Helium, oxygen, proton, and electron (HOPE) mass spectrometer for the radiation belt storm probes mission. *Space Science Reviews*, *179*(1-4), 423–484. https://doi.org/10.1007/s11214-013-9968-7

Kennel, C. (1966). Low-frequency whistler mode. *Physics of Fluids*, *9*(11), 2190–2202. https://doi.org/10.1063/1.1761588

Kennel, C. F., & Petschek, H. E. (1966). Limit on stably trapped particle fluxes. *Journal of Geophysical Research*, *71*(1), 1–28. https://doi.org/10.1029/JZ071i001p00001

Kletzing, C. A., Kurth, W. S., Acuna, M., MacDowall, R. J., Torbert, R. B., Averkamp, T., et al. (2013). The Electric and Magnetic Field Instrument Suite and Integrated Science (EMFISIS) on RBSP. *Space Science Reviews*, *179*(1-4), 127–181. https://doi.org/10.1007/s11214-013-9993-6

Kozyra, J. U., Cravens, T. E., Nagy, A. F., Fontheim, E. G., & Ong, R. S. B. (1984). Effects of energetic heavy ions on electromagnetic ion cyclotron wave generation in the plasmapause region. *Journal of Geophysical Research*, *89*(A4), 2217–2233. https://doi.org/10.1029/JA089iA04p02217

Kurth, W. S., De Pascuale, S., Faden, J. B., Kletzing, C. A., Hospodarsky, G. B., Thaller, S., & Wygant, J. R. (2015). Electron densities inferred from plasma wave spectra obtained by the Waves instrument on Van Allen Probes. *Journal of Geophysical Research: Space Physics*, *120*, 904–914. https://doi.org/10.1002/2014JA020857

Lee, D.-Y., Noh, S.-J., Choi, C.-R., Lee, J. J., & Hwang, J. A. (2017). Effect of hot anisotropic He^+ ions on the growth and damping of electromagnetic ion cyclotron waves in the inner magnetosphere. *Journal of Geophysical Research: Space Physics*, *122*, 4935–4942. https://doi.org/10.1002/2016JA023826

Liu, Y. H., Fraser, B. J., & Menk, F. W. (2012). Pc2 EMIC waves generated high off the equator in the dayside outer magnetosphere. *Geophysical Research Letters*, *39*, L17102. https://doi.org/10.1029/2012GL053082

Loto'aniu, T. M., Fraser, B. J., & Waters, C. L. (2005). Propagation of electromagnetic ion cyclotron wave energy in the magnetosphere. *Journal of Geophysical Research*, *110*, A07214. https://doi.org/10.1029/2004JA010816

Min, K., Lee, J., Keika, K., & Li, W. (2012). Global distribution of EMIC waves derived from THEMIS observations. *Journal of Geophysical Research*, *117*, A05219. https://doi.org/10.1029/2012JA017515

Min, K., & Liu, K. (2016). Proton velocity ring-driven instabilities in the inner magnetosphere: Linear theory and particle-in-cell simulations. *Journal of Geophysical Research: Space Physics*, *121*, 475–491. https://doi.org/10.1002/2015JA022042

Min, K., Liu, K., Bonnell, J. W., Breneman, A. W., Denton, R. E., Funsten, H. O., et al. (2015). Study of EMIC wave excitation using direct ion measurements. *Journal of Geophysical Research: Space Physics*, *120*, 2702–2719. https://doi.org/10.1002/2014JA020717

Nosé, M., Takahashi, K., Anderson, R. R., & Singer, H. J. (2011). Oxygen torus in the deep inner magnetosphere and its contribution to recurrent process of O^+-rich ring current formation. *Journal of Geophysical Research*, *116*, A10224. https://doi.org/10.1029/2011JA016651

Olsen, R. C., Shawhan, S. D., Gallagher, D. L., Green, J. L., Chappell, C. R., & Anderson, R. R. (1987). Plasma observations at the Earth's magnetic equator. *Journal of Geophysical Research*, *92*(A3), 2385–2407. https://doi.org/10.1029/JA092iA03p02385

Saikin, A. A., Zhang, J.-C., Allen, R. C., Smith, C. W., Kistler, L. M., Spence, H. E., et al. (2015). The occurrence and wave properties of H^+-, He^+-, and O^+-band EMIC waves observed by the Van Allen Probes. *Journal of Geophysical Research: Space Physics*, *120*, 7477–7492. https://doi.org/10.1002/2015JA021358

Santolík, O., Parrot, M., & Lefeuvre, F. (2003). Singular value decomposition methods for wave propagation analysis. *Radio Science*, *38*(1), 1010. https://doi.org/10.1029/2000RS002523

Usanova, M. E., Drozdov, A., Orlova, K., Mann, I. R., Shprits, Y., Robertson, M. T., et al. (2014). Effect of EMIC waves on relativistic and ultrarelativistic electron populations: Gound-based and Van Allen Probes observations. *Geophysical Research Letters*, *41*, 1375–1381. https://doi.org/10.1002/2013GL059024

Wygant, J. R., Bonnell, J. W., Goetz, K., Ergun, R. E., Mozer, F. S., Bale, S. D., et al. (2013). The Electric Field and Waves (EFW) instruments on the Radiation Belts Storm Probes mission. *Space Science Reviews*, *179*(1-4), 183–220. https://doi.org/10.1007/s11214-013-0013-7

Xue, S., Thorne, R. M., & Summers, D. (1993). Electromagnetic ion-cyclotron instability in space plasmas. *Journal of Geophysical Research*, *98*(A10), 17,475–17,484. https://doi.org/10.1029/93JA00790

Yu, X., Yuan, Z., Huang, S., Wang, D., Li, H., Qiao, Z., & Yao, F. (2017). EMIC waves covering wide L shells: MMS and Van Allen Probes observations. *Journal of Geophysical Research: Space Physics*, *122*, 7387–7395. https://doi.org/10.1002/2017JA023982

Yu, X., Yuan, Z., Wang, D., Huang, S., Qiao, Z., Yu, T., & Yao, F. (2016). Excitation of oblique O+ band EMIC waves in the inner magnetosphere driven by hot H^+ with ring velocity distributions. *Journal of Geophysical Research: Space Physics*, *121*, 11,101–11,112. https://doi.org/10.1002/2016JA023221

Yu, X., Yuan, Z., Wang, D., Li, H., Huang, S., Wang, Z., et al. (2015). In situ observations of EMIC waves in O^+ band by the Van Allen Probe A. *Geophysical Research Letters*, *42*, 1312–1317. https://doi.org/10.1002/2015GL063250

Yuan, Z., Deng, X., Lin, X., Pang, Y., Zhou, M., Décréau, P. M. E., et al. (2010). Link between EMIC waves in a plasmaspheric plume and a detached sub-auroral proton arc with observations of Cluster and IMAGE satellites. *Geophysical Research Letters*, *37*, L07108. https://doi.org/10.1029/2010GL042711

Yuan, Z., Xiong, Y., Pang, Y., Deng, X., Trotignon, J. G., Lucek, E., & Wang, J. (2012). Wave-particle interaction in a plasmaspheric plume observed by a Cluster satellite. *Journal of Geophysical Research*, *117*, A03205. https://doi.org/10.1029/2011JA017152

Yuan, Z., Li, M., Xiong, Y., Li, H., Zhou, M., Wang, D., et al. (2013). Simultaneous observations of precipitating radiation belt electrons and ring current ions associated with the plasmaspheric plume. *Journal of Geophysical Research: Space Physics*, *118*, 4391–4399. https://doi.org/10.1002/jgra.50432

Yuan, Z., Xiong, Y., Huang, S., Deng, X., Pang, Y., Zhou, M., et al. (2014). Cold electron heating by EMIC waves in the plasmaspheric plume with observations of the Cluster satellite. *Geophysical Research Letters*, *41*, 1830–1837. https://doi.org/10.1002/2014GL059241

Yuan, Z., Yu, X., Huang, S., Wang, D., & Funsten, H. O. (2017). In situ observations of magnetosonic waves modulated by background plasma density. *Geophysical Research Letters*, *44*, 7628–7633. https://doi.org/10.1002/2017GL074681

Yuan, Z., Yu, X., Wang, D., Huang, S., Li, H., Yu, T., et al. (2016). In situ evidence of the modification of the parallel propagation of EMIC waves by heated He^+ ions. *Journal of Geophysical Research: Space Physics*, *121*, 6711–6717. https://doi.org/10.1002/2016JA022573

Zhang, J.-C., Kistler, L. M., Mouikis, C. G., Dumlop, M. W., Klecker, B., & Sauvaud, J.-A. (2010). A case study of EMIC wave-associated He^+ energization in the outer magnetosphere: Cluster and Double Star 1 observations. *Journal of Geophysical Research*, *115*, A06212. https://doi.org/10.1029/2009JA014784